Optical heterodyne spectroscopy of $^{127}I_2$ resonance at 633-nm enhanced by an external optical cavity

Fumio Murakami

Laboratory, Japan Radio Co.,Ltd., 2-1-4, Fukuoka, Kamifukuoka-shi, Saitama, 356, JAPAN

and

Tatehisa Ohta

Faculty of Engineering, Doshisha University, 1-3, Tadara-Miyakodani, Tanabe-cho, Tuzuki-gun, Kyoto, JAPAN

ABSTRACT

Saturation spectroscopy of the $^{127}I_2$ resonance at 633-nm enhanced by an external optical cavity have been studied. Hyperfine components of the R(127) and P(33) lines were detected by using frequency-modulation spectroscopy. The frequency separations of *a* to *h* components of the P(33) line were measured with respect to the *i* component of the R(127) line.

1. Introduction

This paper describes saturation spectroscopy of iodine at 633-nm wavelength which uses commercially available, hard-sealed He-Ne laser and external cell configulation.[1,2] In the present scheme, frequency-modulation spectroscopy[3,4] is employed to detect Doppler-free absorption lines, while saturation beam is enhanced in the optical cavity.[5]

2. Experimental Setup

Figure 1 shows the experimental setup of the system. The laser source is an internal-mirror He-Ne laser which supports two orthogonally polarized modes. The total output power of the laser is 2 mW. The cavity length of the laser is controlled by manipulating the current of a heater wound around the tube so that the intensity difference between two orthogonally polarized modes coincides with a reference signal. By adjusting the reference signal, the frequencies of the modes can be tuned within ±700 MHz around the atomic resonance frequency of the ^{20}Ne. One of these modes is selected by a polarizing beamsplitter (PBS) and split into pump-beam and probe-beam. The iodine cell is placed inside the external ring resonator so that the pumping power is built up resulting in saturated absorption. Polarization anisotropy of the Brewster window of the cell is utilized to keep the cavity in resonance with the laser frequency.[6] To eliminate the Doppler background, the pump beam was intensity-modulated through an acousto-optic modulator (AOM) at the frequency of 20 kHz then coupled into the ring resonator. The probe-beam is frequency-modulated by an electro-optic modulator (EOM) at the frequency of 5 MHz and propagates opposite to the pump-beam in the iodine cell. A beat signal of 5 MHz generated by the saturated absorption is detected by a RF mixer and the intensity-modulated component in the signal is synchronously demodulated by a lock-in amplifier.

3. Results

Figure 2 shows the hyperfine components profile of the R(127) and P(33) lines detected by the system described above. While the frequency of the laser is locked to *a* to *h* component of the P(33) line one by one, the beat frequencies between the laser and the intra-cavity iodine stabilized He-Ne laser (Nikon NN-1) which is locked to the *i* component of the R(127) line are measured.

Table 1 shows the measured frequency separations. The values reported by Morinaga[7] are also listed. The *a* component of P(33) line is separated by 393.5 MHz from the *i* component of the R(127) line. The results agree well with previously reported data. The frequency stability is better than 3×10^{-13} in an integration time of 10^3 sec.

4. References

1. F. Murakami, K. Narumi, and T. Ohta, Proc. SPIE, **1837** (1992) 49.
2. F. Murakami, Y. Shoji, M. Tsukuda, and T. Ohta, Technical digest of CLEO **15** (1995) CWF19.
3. G. C. Bjorklund, Opt. Lett., **5** (1980) 15.
4. J. L. Hall, L. Hollberg, T. Baer, and H. G. Robinson, Appl. Phys. Lett. **39** (1981) 680.
5. M. Long-sheng and J. L. Hall, IEEE J. Quantum Electron. **QE-26** (1990) 2006.
6. T. W. Hansch and B. Couillaud, Opt. Commun., **35** (1980) 441.
7. A. Morinaga, Bulletin of NRLM, **32** (1983) 181.

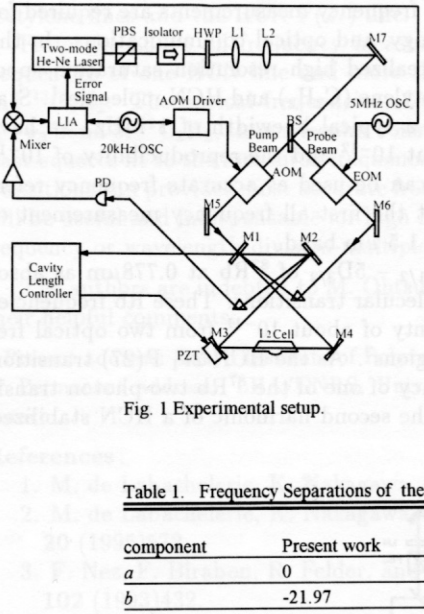

Fig. 1 Experimental setup.

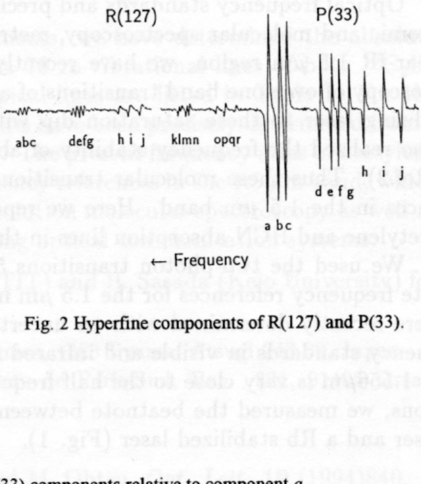

Fig. 2 Hyperfine components of R(127) and P(33).

Table 1. Frequency Separations of the P(33) components relative to component *a*.

		Frequency Separations	
component	Present work	Ref. 7(Calculation)	Ref. 7(Experiment)
a	0	0	0
b	-21.97	-21.95	-22.0
c	-36.67	-36.73	-36.8
d	-118.18	-118.16	-118.2
e	-153.91	-153.88	-153.9
f	-179.29	-179.27	-179.2
g	-214.49	-214.51	-214.5
h	-262.74	-263.50	-263.5